Analytica Chimica Acta 1248 (2023) 340938

Contents lists available at ScienceDirect

Analytica Chimica Acta

journal homepage: www.elsevier.com/locate/aca

Fast and visual detection of nucleic acids using a one-step RPA-CRISPR detection (ORCD) system unrestricted by the PAM

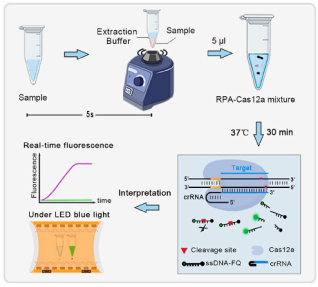
Kangfeng Lin [a,1], Jianguang Guo [a,1], Xiangju Guo [a,1], Qinghan Li [a], Xiao Li [a], Zhen Sun [a], Zehang Zhao [a], Jiao Weng [a], Jinzhun Wu [c,**], Rui Zhang [b,***], Boan Li [a,*]

[a] State Key Laboratory of Cellular Stress Biology, Innovation Center for Cell Signaling Network and Engineering Research Center of Molecular Diagnostics of the Ministry of Education, School of Life Sciences, Xiamen University, Xiamen, Fujian, China
[b] Xiamen Cell Therapy Research Center, The First Affiliated Hospital of Xiamen University, School of Medicine, Xiamen University, Xiamen, 361003, China
[c] Women and Children's Hospital, School of Medicine, Xiamen University, NO.10 Zhenhai Road, Siming District, Xiamen, Fujian, 361003, China

HIGHLIGHTS

- A rapid and visualized one-step detection system of RPA-Cas12 was established.
- The detection system gets rid of the limitation of PAM sequence.
- The higher the activity of Cas12a, the more inhibited the one-step detection system.
- The system can perform nucleic acid extraction and detection of pertussis clinical samples and SARS-COV-2 clinical samples within 30 min.

GRAPHICAL ABSTRACT



ARTICLE INFO

Handling Editor: Dr. J.P. Landers

Keywords:
One-step detection
CRISPR/Cas12a-based detection
PAM sequence
SARS-CoV-2
Visual detection

ABSTRACT

CRISPR-Cas12a (Cpf1) is widely used for pathogen detection. However, most Cas12a nucleic acid detection methods are limited by a PAM sequence requirement. Moreover, preamplification and Cas12a cleavage are separate. Here, we developed a one-step RPA-CRISPR detection (ORCD) system unrestricted by the PAM sequence with high sensitivity and specificity that offers one-tube, rapid, and visually observable detection of nucleic acids. In this system, Cas12a detection and RPA amplification are performed simultaneously, without separate preamplification and product transfer steps, and 0.2 copies/μL of DNA and 0.4 copies/μL of RNA can be detected. In the ORCD system, the activity of Cas12a is the key to the nucleic acid detection; specifically, reducing Cas12a activity increases the sensitivity of ORCD assay detection of the PAM target. Furthermore, by combining this detection technique with a nucleic acid extraction-free method, our ORCD system can be used to extract, amplify and detect samples within 30 min, as verified with tests of 82 *Bordetella pertussis* clinical samples

* Corresponding author.
** Corresponding author.
*** Corresponding author.
E-mail addresses: 1923731201@qq.com (J. Wu), raissarui@foxmail.com (R. Zhang), bali@xmu.edu.cn (B. Li).
[1] These authors contributed equally to this work. Author order was determined on the basis of seniority.

https://doi.org/10.1016/j.aca.2023.340938
Received 9 October 2022; Received in revised form 8 January 2023; Accepted 2 February 2023
Available online 3 February 2023
0003-2670/© 2023 The Authors. Published by Elsevier B.V. This is an open access article under the CC BY license (http://creativecommons.org/licenses/by/4.0/).

with a sensitivity and specificity of 97.30% and 100% compared with PCR. We also tested 13 SARS-CoV-2 samples with RT-ORCD, and the results were consistent with RT–PCR.

1. Introduction

In recent decades, respiratory infectious diseases caused by the gram-negative bacterial pathogens *Bordetella pertussis* (*B. pertussis*) [1], influenza viruses [2,3], severe acute respiratory syndrome-coronavirus (SARS-CoV) [4], and SARS-CoV-2 (previously named 2019-nCoV) [5,6] have seriously threatened human health, especially the outbreak of coronavirus disease 2019 (COVID-19) in 2019 [7]. As of 1 April 2022, according to the World Health Organization (WHO) [8], a total of 486, 761, 597 confirmed cases of COVID-19 had been reported worldwide, and 6,142,735 deaths have been attributed to COVID-19. Therefore, the rapid, early and accurate detection of nucleic acids is of great significance for the diagnosis of diseases, evaluation of treatment plans, formulation of preventive measures, assessment of drug resistance, etc., which in turn can prevent the risk of disease transmission.

The traditional polymerase chain reaction (PCR) or reverse-transcription PCR (RT–PCR) method is the gold standard for nucleic acid detection [9,10], but it is not suitable for simple, rapid and immediate point of care (POC) molecular diagnosis because it usually depends on complex and precise instrumentation and specially trained personnel and involves a long reaction time (approximately 2 h) [11]. To circumvent the limitations of traditional PCR, many isothermal amplification methods, such as recombinase polymerase amplification (RPA) [12,13] and loop-mediated isothermal amplification (LAMP) [14], have been developed. However, these isothermal amplification methods are not suitable for molecular detection because their sensitivity is lower than traditional PCR and can render false-positive results [15–17].

The RNA-guided class 2 clustered regularly interspaced short palindromic repeats/CRISPR-associated proteins (CRISPR/Cas) systems are widely used for molecular diagnosis because of their high rate of collateral cleavage of single-strand DNA (ssDNA) [18,19], such as that induced by Cas12a (previously known as Cpf1) and Cas12 b (previously known as C2c1), which recognize ssDNA or double-stranded (dsDNA), and Cas13a (previously known as C2c2), which recognizes RNA [20–29]. After preamplification, Cas13 and Cas12 nucleases have been developed for use in a variety of nucleic acid detection systems with high specificity and sensitivity, respectively. For example, specific high-sensitivity enzymatic reporter unlocking (SHERLOCK) [30] combined with recombinase-mediated polymerase nucleic acid pre-amplification by the Cas13 nuclease for rapid detection of nucleic acids, DNA endonuclease-targeted CRISPR trans reporter (DETECTR) [31] combined with isothermal amplification of Cas12a nuclease for DNA detection, and one-HOur Low-cost Multipurpose highly Efficient System (HOLMES) [32] combined with PCR preamplification of Cas12a for fast detection of target DNA and target RNA. However, these CRISPR/Cas-based detection strategies, with CRISPR RNAs (crRNAs) that restricted by the protospacer adjacent motif site (PAM) sequence, usually need to be carried out step by step, requiring that first nucleic acid be pre-amplified followed by amplified products transfer to the CRISPR/Cas system for nucleic acid detection [33,34]. This multistep reaction method is not only cumbersome and time consuming but is also easily affected by aerosol contamination. HOLMES has been further developed into a one-step HOLMESv2 method based on Cas12 b and LAMP to address this issue. However, it is less sensitive than qPCR and requires a total reaction time of nearly 2 h [24]. Since the outbreak of SARS-CoV-2, Cas12a has developed rapidly in the field of nucleic acid detection. For example, a visual detection based on Cas12a, AIOD-CRISPR [35], a CRISPR-based point-of-care diagnosis assay, miSHERLOCK [36], an assay using suboptimal protospacer adjacent motifs for Cas12a, sPAMc [37].

In this study, we also propose a one-step RPA-CRISPR detection (ORCD) system unrestricted by the PAM sequence to achieve highly sensitive and specific one-tube, rapid (30 min), and visual detection of nucleic acids. In this ORCD system, the nucleic acid amplification and CRISPR/Cas12a cleavage of a ssDNA reporter are performed simultaneously, which enables the detection of a few copies of the target nucleic acids (DNA or RNA). Furthermore, we reveal that the *cis*-cleavage activity of Cas12a is the key to the detection of nucleic acids by the ORCD system, and the limit of detection (LoD) of the ORCD system for targeting a PAM sequence is greatly improved by reducing the relative Cas12a activity. In addition, after using a nucleic acid-free extraction method, we applied the ORCD system to detect 82 DNA clinical samples of *Bordetella pertussis* with sensitivity and specificity of 97.30% and 100% respectively. We also used the RT-ORCD system to detect 13 RNA clinical samples of SARS-CoV-2 and obtained results consistent with those of the PCR or RT–PCR methods.

2. Materials and methods

2.1. Materials

All DNA templates and primers were synthesized by GENERAL BIOL (Anhui) Co., Ltd. (China). The ssDNA-FQ reporter was synthesized by Sangon Biotechnology Co., Ltd. (Shanghai, China). All sequences and plasmids used in this study are listed in Supplementary Tables 4 and 5 of the Supporting Information. A TwistAmp basic kit was purchased from TwistDx Inc. (Cambridge, UK). The dsDNAs were purified using a TIANprep Midi plasmid kit from Qiagen (Shanghai, China). The PCR amplification products were recovered, and RPA amplification products were extracted using a FastPure Gel DNA Extraction Mini Kit from Vazyme (Nanjing, China). A viral nucleic acid extraction-free release agent kit was provided by BioDetect (Xiamen, China). MutiScript II Reverse Transcriptase was ordered from Fapon Biotech Inc. (Shenzhen, China). A HiScribe T7 Quick High Yield RNA synthesis kit and DNase I (RNase-free) were purchased from New England Biolabs (Beijing, China). Ni sepharose was purchased from GE Healthcare. The *B. pertussis* nucleic acid detection kit (PCR-Fluorescence Probing) used to compare the results with those obtained by ORCD was purchased from Shenzhen YILIFANG Biological Co., Ltd. (Shenzhen, China). The novel coronavirus (2019-nCoV) nucleic acid diagnostic kit (PCR-Fluorescence Probing) used to compared the results with those obtained by RT-ORCD was purchased from Sansure Biotech (Changsha, China). The clinical samples of *B. pertussis* were provided by Beijing Children's Hospital Affiliated to Capital Medical University, and the SARS-COV-2 swab samples were provided by Xiamen Centers for Disease Control and Prevention.

2.2. Preparation of crRNAs

First, the synthesized upstream and downstream oligonucleotides with the T7 promoter sequence, a spacer and a repeat sequence were annealed in 1x annealing buffer containing 50 mM HEPES (pH 7.4) and 100 mM NaCl. Next, the annealed dsDNAs were used as templates for synthesizing crRNA overnight with the HiScribe T7 Quick High Yield RNA synthesis kit at 37 °C. Then, DNase I was added to the transcription system, incubated at 37 °C for 30 min to remove template DNA, and incubated at 85 °C for 10 min to denature it. Finally, the transcribed RNA was purified by a phenol chloroform extraction method and quantified with a NanoDrop 2000C spectrophotometer (Thermo Fisher).

2.3. Preparation of target DNAs and RNAs

The 643-bp PAM-target sequence was inserted into a pUC-57 vector to form the plasmid template. On the basis of the PAM-target plasmid, three TTT bases were removed to obtain a 640-bp non-PAM-target sequence template. No PAM target was derived from IS1663 of Bordetella pertussis (GenBank accession CP046995.1), and the PAM target was a mutant of IS1663. For the SARS-COV-2 target, the sequence containing the T7 promoter and 1260-bp N gene from 28,274 to 29,533 in the SARS-CoV-2 genome (GenBank accession MT322424.1) was inserted into a pUC-57 vector. The target RNAs were transcribed from plasmids carrying T7-promoter-tagged sequences using a HiScribe T7 Quick High Yield RNA synthesis kit. First, a PCR step was performed with a synthetic gene fragment containing a T7-promoter-tagged PCR forward primer and a reverse primer containing the corresponding target sequence. Next, the PCR products were used as templates for synthesizing target RNAs overnight through transcription reactions at 37 °C after recovery with a FastPure Gel DNA Extraction Mini Kit. Then, DNase removal of DNA and phenol chloroform purification of RNA steps were performed to purify crRNA.

2.4. Purification of the LbCas12a protein

The sequence of the LbCas12a protein was optimized on the basis of its expression level and synthesized by General Biological Co., Ltd., and then cloned into the pET32a vector with a 6x His tag in the N-terminus. The recombinant LbCas12a protein was expressed in *E. coli* BL21 (DE3). The cells were grown at 37 °C to an optical density measured at 600 nm (OD600) of 0.6 before expression was induced with 1 mM IPTG treatment at 25 °C for 6 h. Cell pellets were resuspended in 80 mL of lysis buffer (50 mM Tris-HCl (pH 8.0), 0.5 M NaCl, 5 mM DTT, 5% glycerol, and 0.1% Triton X-100). Once homogenized, the cells were lysed by sonication (40% kHz for 21 min) and then centrifuged (12,000 rpm for 30 min at 4 °C), and the supernatant was retained. The supernatant was incubated with Ni sepharose (GE Healthcare), which was preequilibrated in lysis buffer. Then, the column was washed with washing buffer (50 mM Tris-HCl (pH 8.0), 0.5 M NaCl, 5 mM DTT, 5% glycerol, 0.1% Triton X-100, and 50 mM imidazole), and the LbCas12a protein was eluted with elution buffer (50 mM Tris-HCl (pH 8.0), 0.5 M NaCl, 5 mM DTT, 5% glycerol, 0.1% Triton X-100, and 250 mM imidazole). The eluted fractions containing LbCas12a were collected and dialyzed overnight into storage buffer (20 mM Tris-HCl (pH 8.0), 0.5 M NaCl, 5 mM DTT, and 1 mM EDTA). After dialysis, the fractions containing LbCas12a were concentrated to a final concentration of 2 mg/mL and stored at −20 °C with the addition of 50% glycerol.

2.5. Cis-cleavage assay

Cis-cleavage was performed with the LbCas12a protein at 37 °C in cleavage buffer containing 50 mM Tris-HCl (pH 7.9), 100 mM NaCl, 10 mM $MgCl_2$ and 1 mM DTT. The cleavage reaction consumed 0.496 μM synthesized crRNA and 200 ng of target DNA in plasmids or PCR amplicons. The sample was then analyzed in a 1% agarose gel. ImageJ software was used to analyze the results.

2.6. Trans-cleavage assay

The *trans*-cleavage assay was carried out by cleaving the ssDNA-FQ reporter. The reaction mixture contained LbCas12a, 0.496 μM crRNA, 2 μM ssDNA-FQ reporter and 200 ng of the target DNA and was carried out in a SLAN-96 P real-time PCR instrument (Shanghai Hongshi Medical Technology Co., Ltd.). The fluorescence intensity was measured every minute for 30 min. After 30 min, the sample was scanned image capture using a THBC-470 LED blue light (TUOHE) and Clinx Gel Documentation System (Clinx).

2.7. ORCD assay

The ORCD assay was performed simultaneously in one tube containing RPA amplification and Cas12a cleavage reaction mixtures. Specifically, the 25-μL one-tube reaction assay contained 6.25 μL of concentrated buffer A (25% PEG20000), 1.25 μL of buffer B (240 mM Magnesium acetate), 0.32 μM primer (for each primer), 0.8 μM dNTP, 0.46 μM LbCas12a, 0.496 μM crRNA, 2 μM ssDNA-FQ reporter (5′-FAM-TCCCT-BHQ-3′) and 5 μL of the target DNA. Except that RT-ORCD system contains 0.32U/μL MutiScript II reverse transcriptase, the components of RT-ORCD were mostly consistent with those of ORCD. Real-time fluorescence detection was performed with a SLAN-96 P real-time PCR instrument. The fluorescence intensity was measured every 1 min for 30 min while the PCR was running. After the ORCD reaction mixture was incubated for 30 min at 37 °C, the tube was inspected under LED blue light and UV light.

2.8. The nucleic acid extraction-free release agent method

The viral nucleic acid extraction-free release agent kit was used to extract DNA or RNA from clinical samples. Specifically, for DNA extraction, 20 μL of liquid samples was added to the same volume of nucleic acid extraction buffer. 5 U/μL RNase inhibitor was added after extracting the RNA samples. After shaking for 5 s, the lysed sample was used as the template for amplification.

3. Results and discussion

3.1. crRNA/LbCas12a showed weaker cis-cleavage activity and similar trans-cleavage activity with non-PAM target than with PAM targets

We purified LbCas12a (*Lachnospiraceae bacterium* ND2006 Cas12a) and confirmed that LbCas12a had both *cis*-cleavage activity on dsDNA and collateral *trans*-cleavage activity on ssDNA (Supplementary Fig. 1). Consistent with previous findings, the PAM site of 5′-TTTN-3′ was required by LbCas12a to cleave target dsDNA [25,38]. To investigate the cleavage activity of Cas12a on dsDNA without strict PAM recognition restriction, we designed a crRNA with a 20-nucleotide (nt) sequence targeting a PAM and non-PAM dsDNA template. As shown in Fig. 1a, the non-PAM target sequence was derived from the IS1663 sequence of *Bordetella pertussis*, which differed from the 5′-TTT-3′ of PAM sequence in three bases. The two sequences were completely identical except for the PAM sequence and paired with crRNA targeting.

To evaluate the performance of crRNA targeting of the non-PAM sequence, we first tested the *cis*-cleavage activity of crRNA/Cas12a. PAM-target and non-PAM-target plasmids were used as the templates. As shown in Fig. 1b, crRNA/Cas12a exhibited higher *cis*-cleavage activity with prolonged reaction time. However, the *cis*-cleavage activity of crRNA/Cas12a targeting the non-PAM sequence was weaker than that of the crRNA/Cas12a targeting the PAM sequence, but no significant increase in cleavage was observed after 30 min of incubation. Next, we tested the *trans*-cleavage activity of crRNA/Cas12a. The ssDNA-fluorophore quencher (FQ) reporter used for this experiment was a 5-nt ssDNA (5′-TCCCT-3′) labeled with a 5′-FAM (fluorescein) dye and 3′-black hole quencher. After incubation at 37 °C for 30 min, the real-time fluorescence results showed high crRNA *trans*-cleavage activity when targeting either the PAM or non-PAM sequence, and the fluorescence was saturated within 10 min (Fig. 1c). However, the *trans*-cleavage activity of Cas12a targeted to the PAM sequence was higher, and the fluorescence was saturated in only approximately 3 min, while targeting the non-PAM sequence was achieved in approximately 7 min. In addition, after 30 min of incubation, the fluorescence emitted by cleavage of the targeted PAM and non-PAM sequences was *high* and nearly identical (Fig. 1d) and was directly visualized under an LED blue or ultraviolet (UV) light illuminator (Fig. 1e). These results suggested that crRNA/Cas12a recognizes non-PAM targets and shows weaker *cis*-cleavage and

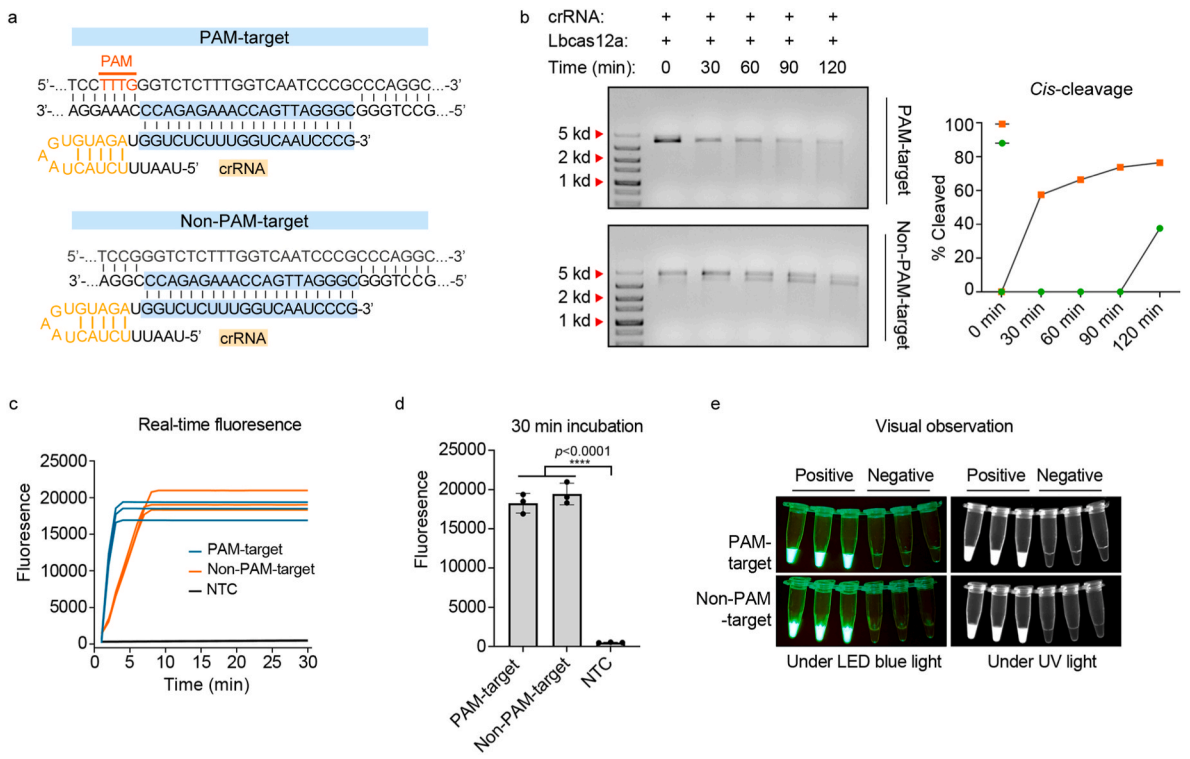


Fig. 1. The *cis* and *trans* cleavage of LbCas12a/crRNA targeted to PAM and non-PAM sequences. a. Schematic of CRISPR RNA (crRNA) targeting a PAM and non-PAM sequence. The PAM sequence, 5′-TTTG-3′, is in red. **b.** The *cis*-cleavage of crRNA/LbCas12a targeting PAM- and non-PAM-containing plasmids at different times. **c, d, e.** The *trans*-cleavage activity of crRNA/LbCas12a targeting PAM- and non-PAM-containing plasmids after incubation for 30 min. The single-stranded DNA with a fluorophore quencher (ssDNA-FQ) was labeled with 5′ FAM (fluorescein) and 3′ BHQ1. NTC, nontemplate control reaction. Error bars represent the means ± S.D. of n = 3 replicates ns = not significant with p > 0.05, and asterisks (*, **, ***, and ****) denote significant differences based on the p values listed above. The source data are available in the source data file. (For interpretation of the references to colour in this figure legend, the reader is referred to the Web version of this article.)

similar *trans*-cleavage activity compared with its effect on dsDNA with PAM sequences.

3.2. Non-PAM-targeted crRNA/LbCas12a enhanced one-step RPA-CRISPR detection (ORCD) assay

Next, we combined crRNA/Cas12a targeting of non-PAM sequences with RPA for nucleic acid detection following the DETECTR method because similar *trans*-cleavage activity was found with the DETECTR method when both the PAM sequence and a non-PAM sequence was targeted. First, the target sequences were pre-amplified by RPA at 37 °C for 10 min, and then the amplified products were transferred to a Cas12a reaction system for fluorescence detection. The results are shown in Supplementary Fig. 2. Whether the PAM or a non-PAM sequence was targeted, 10^4 copies/μL of the target were detected with the DETECTR method; however, the detection efficiency of the targeted PAM sequence was better than that of the non-PAM sequence.

To prevent cap opening, we integrated crRNA/Cas12a and RPA targeting PAM and non-PAM sequences into a single reaction system to establish the ORCD system. Specifically, we directly added the Cas12a system to the RPA reaction solution without preamplification and incubated the solution at 37 °C for 30 min before fluorescence detection. The workflow of the ORCD method is shown in Fig. 2a. All reagents, including the RPA mixture, crRNA/LbCas12a complex and ssDNA ssDNA-FQ reporter, were encapsulated in a single pellet. When Mg^{2+} was added to one pellet containing the ORCD system at 37 °C, RPA amplification was initiated. Then, when the crRNA/Cas12a complexes recognized and bound the target site, the Cas12a endonuclease was activated and cleaved the ssDNA-FQ reporters, generating an intense fluorescence signal, which was directly visualized under an LED blue or a UV light illuminator.

To systematically evaluate our ORCD assay, we prepared and tested 12 systems containing various components (Reactions 1–12) for targeting PAM and non-PAM sequences. A total of 10^4 copies/μL of plasmid containing a 643-bp PAM sequence target and a 640-bp non-PAM target sequence were used (Supplementary Table 4). The crRNA targeted both the PAM and non-PAM DNA templates. In addition, the ssDNA sequence (TCCCT) with the 5-terminus-labeled FAM fluorescent group and the 3-terminus-labeled BHQ1 quenching group was used as reporter molecules, and the change in fluorescence was monitored in real time at 37 °C. As shown in Fig. 2b, surprisingly, only reaction 8, containing the non-PAM-target, reporter molecules, crRNA, LbCas12a, and the RPA reaction mixture, exhibited a significantly increased fluorescence signal, which reached a saturation point at 13 min. In addition, the fluorescence intensity at the end of the reaction for 30 min was directly observable to the naked eye under a LED blue light or ultraviolet radiation (Fig. 2c). In contrast, after incubation of RPA and Cas12a at 37 °C for 30 min, no significant fluorescent signals were observed for reaction 4 targeting the PAM sequence. To explore which types of preamble sequences were more advantageous in one-step method, we tested 64 PAM sequences covering 5′-NNN-3′ sequences by ORCD system. The results showed that the most preferred PAM sequence TTT and targets containing two T (TTN, NTT, TNT) showed poor performance in ORCD, while TCC, TCG, CCT, CTC, GTC and CTG showed excellent activity in ORCD (Supplementary Figs. 3 and 4). These results demonstrate that, in our ORCD assay system, the combination of crRNA/Cas12a not limited to PAM region targeting, and RPA is a simple, rapid and one-tube method for nucleic acid detection, but this outcome differed when the PAM sequence was targeted.

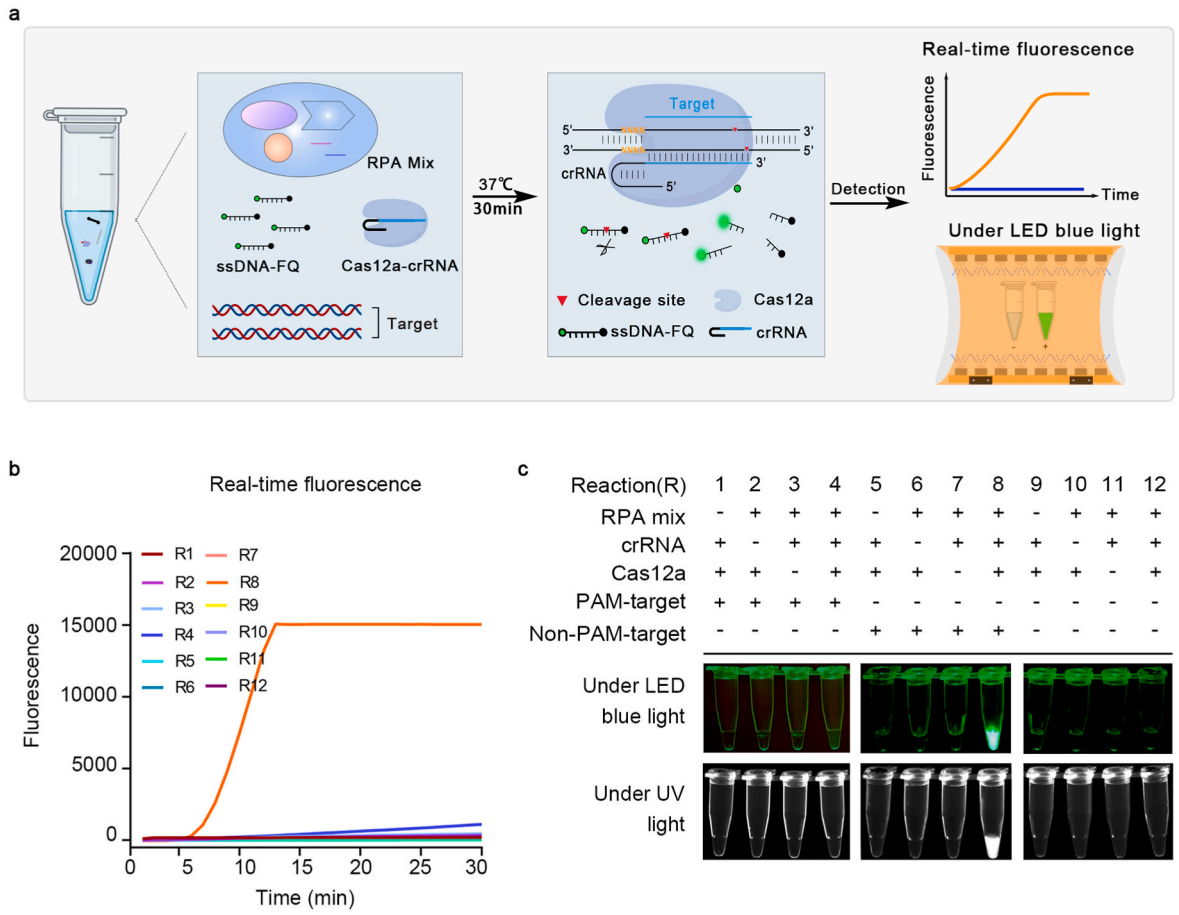


Fig. 2. Workflow of the ORCD assay. a. Schematic showing the ORCD assay system for rapid and visual nucleic acid detection. All reagents were mixed into a single pellet. The reaction was assessed in real time by monitoring the fluorescence signal intensity, and the end-point fluorescence was observed with the naked eye through a LED blue light illuminator. **b, c.** Evaluation of the ORCD system targeting PAM and non-PAM plasmids by real-time fluorescence and endpoint imaging. The ORCD system contained 0.248 μM crRNA, 0.46 μM LbCas12a, 0.8 μM single-stranded DNA with a fluorophore quencher (ssDNA-FQ), 0.32 μM primers, 14 mM MgOAc and a recombinase polymerase amplification (RPA) mixture. The target plasmid concentration was 10^4 copies/μL. Each experiment was repeated three times, and similar results were obtained each time. (For interpretation of the references to colour in this figure legend, the reader is referred to the Web version of this article.)

3.3. Non-PAM-targeted crRNA/LbCas12a enhanced the sensitivity of the ORCD assay

Next, to enhance the sensitivity of the ORCD assay system, we optimized the components of the system. The results showed that the optimal amounts of Cas12a protein, crRNA, ssDNA-FQ reporter and primer were 0.46 μM, 0.744 μM, 1.2 μM, and 0.64 μM, respectively (Supplementary Figs. 5, 6, 7, and 8). In addition, we found that when the optimal amount of Cas12a protein was exceeded, the concentration of the Cas12a nuclease was increased and the fluorescence signals produced by cleavage of the ssDNA-FQ reporter was decreased (Supplementary Fig. 8). When the crRNA, ssDNA-FQ reporter and primers were added at certain concentration ranges, the fluorescence signals emitted after reporter cleavage was high and increased with increasing concentrations until fluorescence saturation was reached (Supplementary Figs. 5, 6, 7).

Under optimal conditions, the sensitivity of the ORCD assay system was evaluated. Seven 10-fold dilution gradients of DNA plasmids with and without the PAM region from *Bordetella pertussis* were used as templates, and each gradient was assayed 5 times using a crRNA that can target both templates. As shown in Fig. 3 and Supplementary Fig. 9, we found that the ORCD assay consistently detected non-PAM-target plasmid DNA when the input was as low as 0.2 copies/μL (Fig. 3a, b, 3c), which indicated must higher sensitivity than that observed for PAM sequence detection, which required a minimum of 20,000 copies/μL of input (Fig. 3d, e, 3f). In addition, we compared the sensitivity of ORCD with that of DETECTR. The real-time fluorescence assay results revealed that the LoD of the DETECTR targeting PAM or non-PAM sequences was 0.2 copies/μL of input (Supplementary Figs. 10 and 11). The sensitivity of our ORCD system targeting non-PAM sequences was equivalent to that of the DETECTR method, but the ORCD sensitivity of PAM target sequences was significantly worse than that of DETECTR. In addition to this high sensitivity, ORCD system showed high specificity in detecting *Bordetella pertussis* within 30 min (Supplementary Fig. 12).

3.4. PAM-targeted crRNA/LbCas12a with lower cis-cleavage activity enhanced the sensitivity of ORCD

We next sought to understand the potential mechanism for the insensitivity of the ORCD system in detecting the PAM sequence. With the ORCD system, the higher the concentration of Cas12a was, the lower the sensitivity of non-PAM sequence detection (Supplementary Fig. 8). We speculate that highly active Cas12a inhibits the RPA amplification. Therefore, we compared the activity of Cas12a targeting of PAM and non-PAM sequences. First, we tested the *cis*-cleavage activity of Cas12a at different concentrations. As shown in Fig. 4a, the *cis*-cleavage activity of crRNA/Cas12a targeting the PAM or non-PAM sequence was increased with increasing Cas12a concentration. In addition, the *cis*-cleavage activity of crRNA/Cas12a targeting the PAM sequence was superior to that targeting the non-PAM sequence at equivalent Cas12a

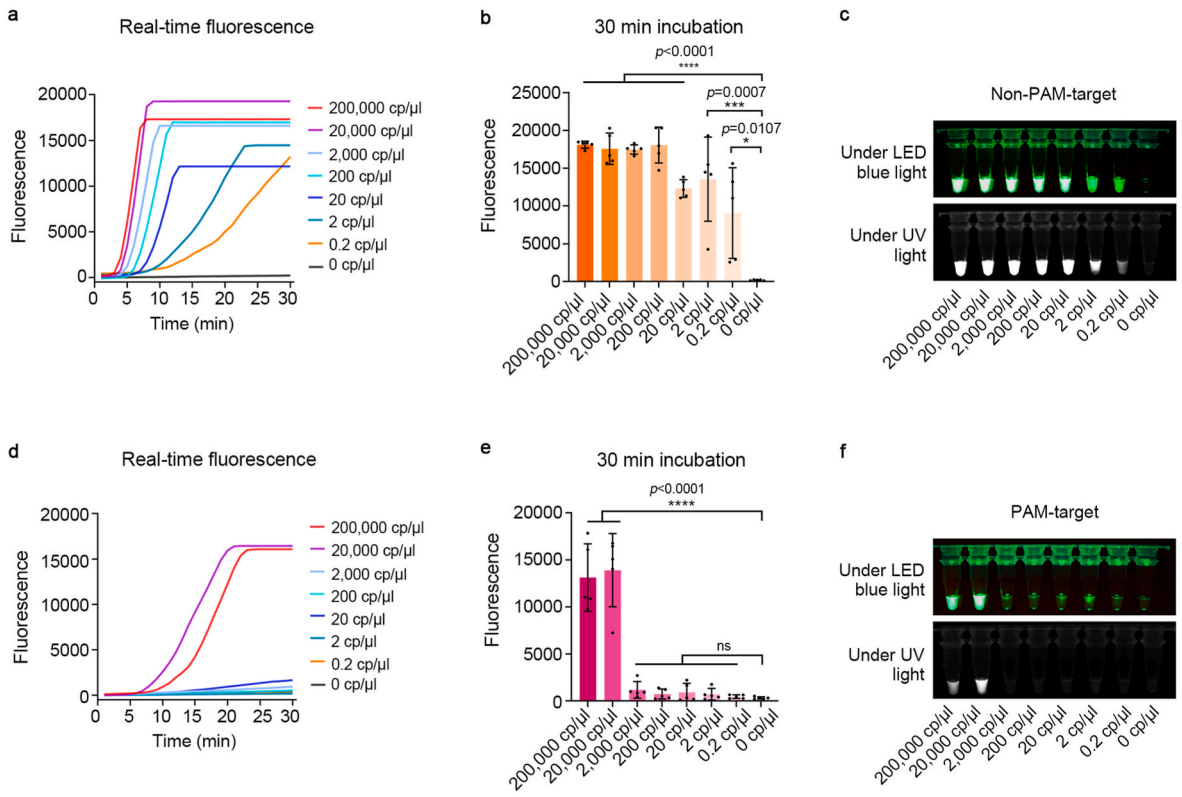


Fig. 3. Sensitivity of the ORCD assay system for the detection of PAM and non-PAM targets. a, b, c. Real-time fluorescence and endpoint imaging results showing the sensitivity of the ORCD system detecting non-PAM targets. The source data are available in the Source Data file. **d, e, f.** Real-time fluorescence and endpoint imaging showing the sensitivity of the ORCD system detecting PAM targets. The source data are available in the Source Data file. Error bars represent the mean ± S.D. with n = 5 replicates. ns = not significant with p > 0.05, and the asterisks (*, **, ***, and ****) denote significant differences with the p values listed above.

concentrations. Then, we tested *trans*-cleavage of Cas12a at different concentrations, and the *trans*-cleavage activity of Cas12a was found to be increased when its concentration was increased (Fig. 4b and Supplementary Fig. 13).

Next, we tested the effects of different Cas12a activity, as measured by concentration, on amplification by the ORCD system targeting the PAM region. Surprisingly, the ORCD system detected 10^4 copies/μL of input PAM target sequences when the Cas12a concentration (e.g., activity) was relatively low (0.23 μM), but when the Cas12a concentration was high, the ORCD system failed to detect the PAM sequence at the 10^4 copies/μL level (Supplementary Fig. 14). Moreover, the sensitivity analysis also showed that the ORCD system consistently detected 20 copies/μL of PAM target input when the Cas12a activity was relatively low (Fig. 4c, d, 4e and Supplementary Fig. 15), which was 10^3 folds higher than that obtained when Cas12a activity was relatively high activity (Fig. 3d, e, 3f). These results demonstrate that Cas12a activity is the key to the detection of nucleic acids by the ORCD system. Cas12a of the ORCD system with low activity exhibited reduced nucleic acid cleavage, which is conducive to greater amplification of RPA and more sensitive detection of low nucleic acid levels.

3.5. *Application of non-PAM-targeted ORCD systems for SARS-CoV-2 detection*

Furthermore, to verify the applicability of the ORCD system, we designed a crRNA not limited to PAM sequence identification to detect the N gene of SARS-CoV-2 (Supplementary Fig. 16) and then used the ORCD system to detect ORCD sensitivity. The real-time fluorescence and endpoint imaging results showed that the LoD was also as low as 0.2 copies/μL of target input (Fig. 5a, b, 5c and Supplementary Fig. 17).

Next, to evaluate the target specificity of ORCD, we tested commercially synthesized plasmids containing the complete N gene in SARS-CoV (accession number NC_004718) and a bat SARS-like coronavirus (bat-SL-CoVZC45, accession number MG772933). The crRNA was designed with one base that did not match the SARS-CoV sequence and two bases that did not match the bat SARS-like coronavirus (Fig. 5d). As shown in Fig. 5e, f, 5g, our ORCD system produced an intense fluorescence signal that was observed either during the real-time analysis or as UV and LED blue light detectable by the naked eye at the end of the experiment only when it was applied to the SARS-CoV-2 plasmid. These results indicate that our developed ORCD assay system exhibits high specificity and does not report cross-reactions with untargeted sequence fragments.

In addition to DNA, RNA targets can be detected with our ORCD assay system, but RNA needs to be reverse transcribed into cDNA before it can be used as the detection template. Therefore, MutiScript II reverse transcriptase was added to the ORCD system to establish a reverse transcription–one-step RPA-CRISPR Detection (RT–ORCD) system to detect RNA. As shown in Supplementary Fig. 18, the PCR product of a SARS-COV-2 N gene fragment containing the T7 promoter was transcribed into RNA by T7 RNA transcriptase and used as the detection template, and our RT-ORCD system consistently detected as few as 0.4 copies/μL of SARS-CoV-2 N RNA target, as determined through real-time fluorescence or naked eye observation (Fig. 5h, i, 5j and Supplementary Fig. 19). However, when detecting PAM target, the sensitivity of RT-ORCD system was 4000 copies/μL, which was far worse than that of non-PAM target (Supplementary Fig. 20). Also, the RT-ORCD assay showed a high specificity in the SARS-CoV-2 detection without any cross-interaction with other sequences (Supplementary Fig. 21).

These results indicate that our ORCD assay method can be used to detect DNA and RNA at single-copy sensitivity. In addition to this high sensitivity, it exhibits specificity and rapid nucleic acid detection, yielding results in approximately 30 min.

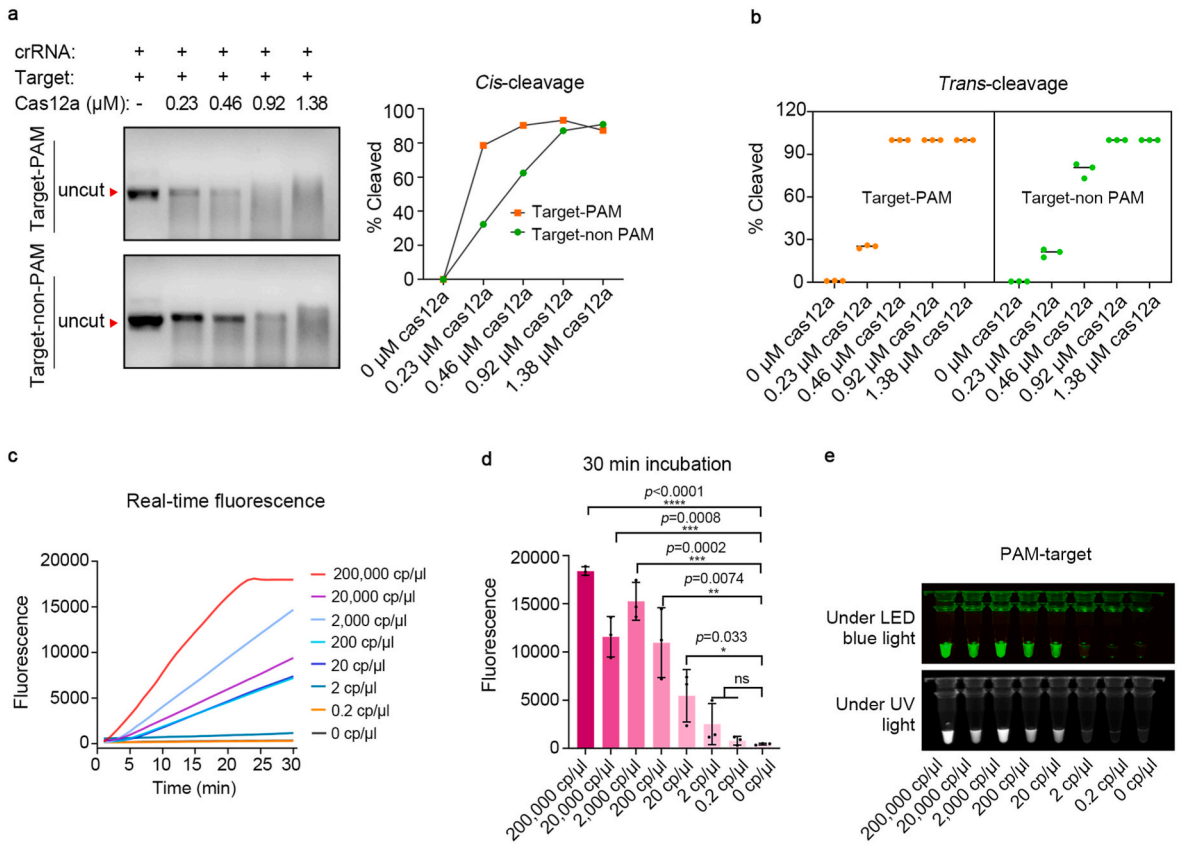


Fig. 4. Cis and *trans* cleavage of LbCas12a at different concentrations and the sensitivity of LbCas12a at low concentrations in detecting PAM target sequences. a. The *cis*-cleavage activity of PAM- and non-PAM-targeting LbCas12a at different concentrations. **b.** The *trans*-cleavage efficiency of PAM- and non-PAM targeting LbCas12a at different concentrations. Three replicates were analyzed (n = 3). Each point represents the mean quantified percentage of sequences cleavage after 30 min at 37 °C, at which time the reaction was completed. The source data are available in the Source Data file**. c, d, e.** Real-time fluorescence and endpoint imaging showing the sensitivity of ORCD for detecting PAM targets when the concentration of LbCas12a was 0.23 μM. The source data are available in the Source Data file. Error bars represent the mean ± S.D. of n = 3 replicates. ns = not significant with p > 0.05, and the asterisks (*, **, ***, and ****) denote significant differences with the p values listed above.

3.6. DNA and RNA clinical samples were rapidly detected by the ORCD (RT-ORCD) system

To facilitate the detection of clinical samples, the ORCD assay system was combined with the nucleic acid extraction-free release agent method, and using this system, nucleic acids were extracted and detected within 30 min. The workflow for rapid nucleic acid extraction and detection is shown in Fig. 6a. Specifically, 20 μL of sample was added to the same volume of nucleic acid extraction buffer. Additional 0.5 U/μL RNase inhibitor was added when RNA sample extraction. After shaking for 5 s, the 5 μL of this lysed sample was added to the ORCD or RT-ORCD system as the amplification target. The results were monitored in real time by fluorescence and with the naked eye by LED blue light and ultraviolet light.

The ORCD assay performed with a nucleic acid extraction-free release agent was further applied to detect *Bordetella pertussis* (*B. pertussis*) in samples of patients with whooping cough. A total of 82 de-identified clinical swab samples (including five whooping cough-positive samples prepared in culture) were tested with our ORCD assay in combination with a nucleic acid extraction-free release agent. In addition, the extracted clinical samples were subjected to real-time fluorescence PCR. As shown in Fig. 6b and Supplementary Fig. 22, 23 and 24, all 19 whooping cough-positive culture samples were identified to be *B. pertussis*-positive by our ORCD system with the nucleic acid extraction-free release agent in 30 min. In addition, 17 whooping cough culture-negative samples were identified as *B. pertussis*-positive with our method, and a total of 36 *B. pertussis*-positive and 46 *B. pertussis*-negative samples were tested. Furthermore, compared with real-time fluorescent PCR (Supplementary Tables 1–2), our ORCD sensitivity and specificity were 97.30% and 100%, respectively. These outcomes showed that our ORCD assay system detected *B. pertussis* with high sensitivity with samples assayed by the clinical gold standard method of isolation and culture and were highly consistent with those of the real-time fluorescence PCR assays. In addition, we tested 13 SARS-COV-2 swab samples with RT-ORCD, including 5 SARS-COV-2-positive and 8 negative samples. From the results of the real-time fluorescence and LED blue or UV light observations (Fig. 6c), the RT-ORCD identified all five positive samples, which were confirmed by RT–PCR to be positive, and correspondingly, the negative samples were confirmed to be negative by RT–PCR (Supplementary Table 3).

4. Conclusion

In this study, we presented a one-step RPA (or RT-RPA)-CRISPR detection strategy for the rapid and visual detection of DNA or RNA by crRNA without a PAM sequence (5′-TTTN-3′). A key advancement with this work is demonstrated by the use of a crRNA that is not strictly restricted by the PAM sequence and that shows similar *trans*-cleavage activity and lower *cis*-cleavage activity to that targeting the PAM sequence within 30 min. Moreover, the high *trans*-cleavage activity is observable with the naked eye through LED blue light or UV light imaging, and therefore, no complex instruments are needed.

The secondary key advance is that the ORCD is a rapid, one-step RPA (or RT-RPA)-CRISPR detection system that can be used to test DNA and

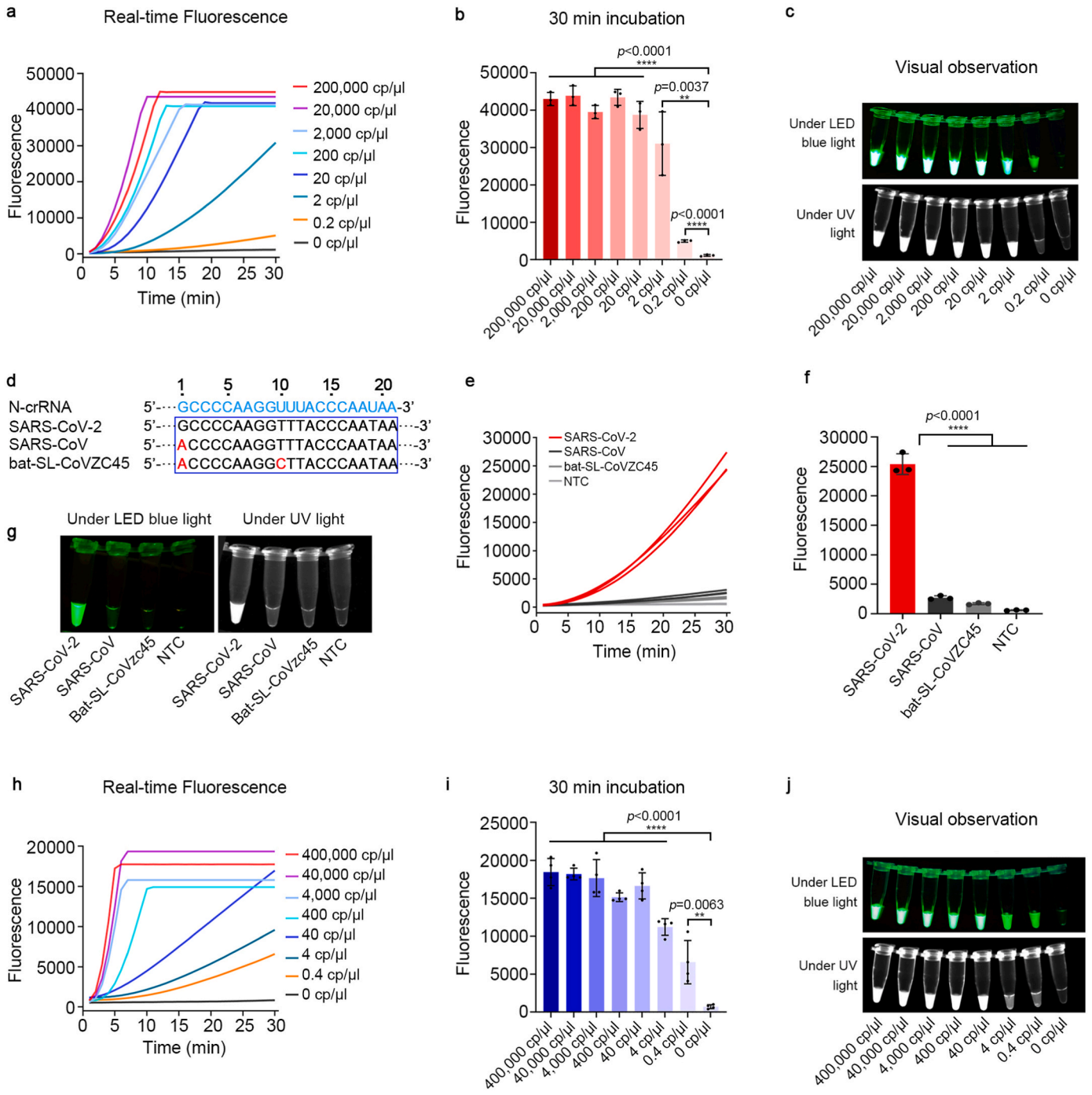


Fig. 5. Specificity and sensitivity and of ORCD and RT-ORCD for the detection of SARS-CoV-2 N gene DNA and RNA sequences. a, b, c. Real-time fluorescence and endpoint imaging results showing the sensitivity of ORCD for detecting SARS-CoV-2 N gene DNA sequences. Three replicates were run (n = 3). The source data are available in the Source Data file. **d.** Alignment of crRNA-targeted sequences of SARS-COV-2 N gene, SARS-COV N and bat-SL-CoVZC45 N gene. **e, f, g.** After sequence alignment, the nucleotide sequences of similar pathogens in the coronavirus family containing SARS-CoV-2 was subjected to ORCD assay, and the real-time fluorescence and endpoint imaging results showing ORCD specificity is presented. The targets included a plasmid harboring the SARS-COV-2 N gene, a plasmid harboring the SARS-COV N gene and a plasmid harboring the bat-SL-CoVZC45 N gene. Three replicates were run (n = 3). **h, i, j.** Real-time fluorescence and endpoint imaging results showing the sensitivity of ORCD in detecting SARS-CoV-2 N gene RNA sequences. Four replicates were run (n = 4). The source data are available in the Source Data file.

RNA with sensitivity and specificity. In the ORCD system, all components, including the RPA (or RT-RPA) mixture and crRNA/LbCas12a mixture, were incubated in one test tube, and fluorescence was detected during amplification. According to recent reports, most COVID-19 detection methods based on isothermal amplification and CRISPR detection require a two-step reaction because of interference caused by isothermal amplification and CRISPR detection performed in one step [33,34]. In this process, isothermal amplification or reverse transcription and isothermal amplification are performed first to amplify the product in a separate step, and then, the product is transferred to a CRISPR/Cas system for fluorescence detection. Moreover, this two-step process requires opening the amplification reaction tube, which increases the risk of cross-contamination and possible false-positive results when clinical samples are tested. In contrast, our ORCD (or RT-ORCD)

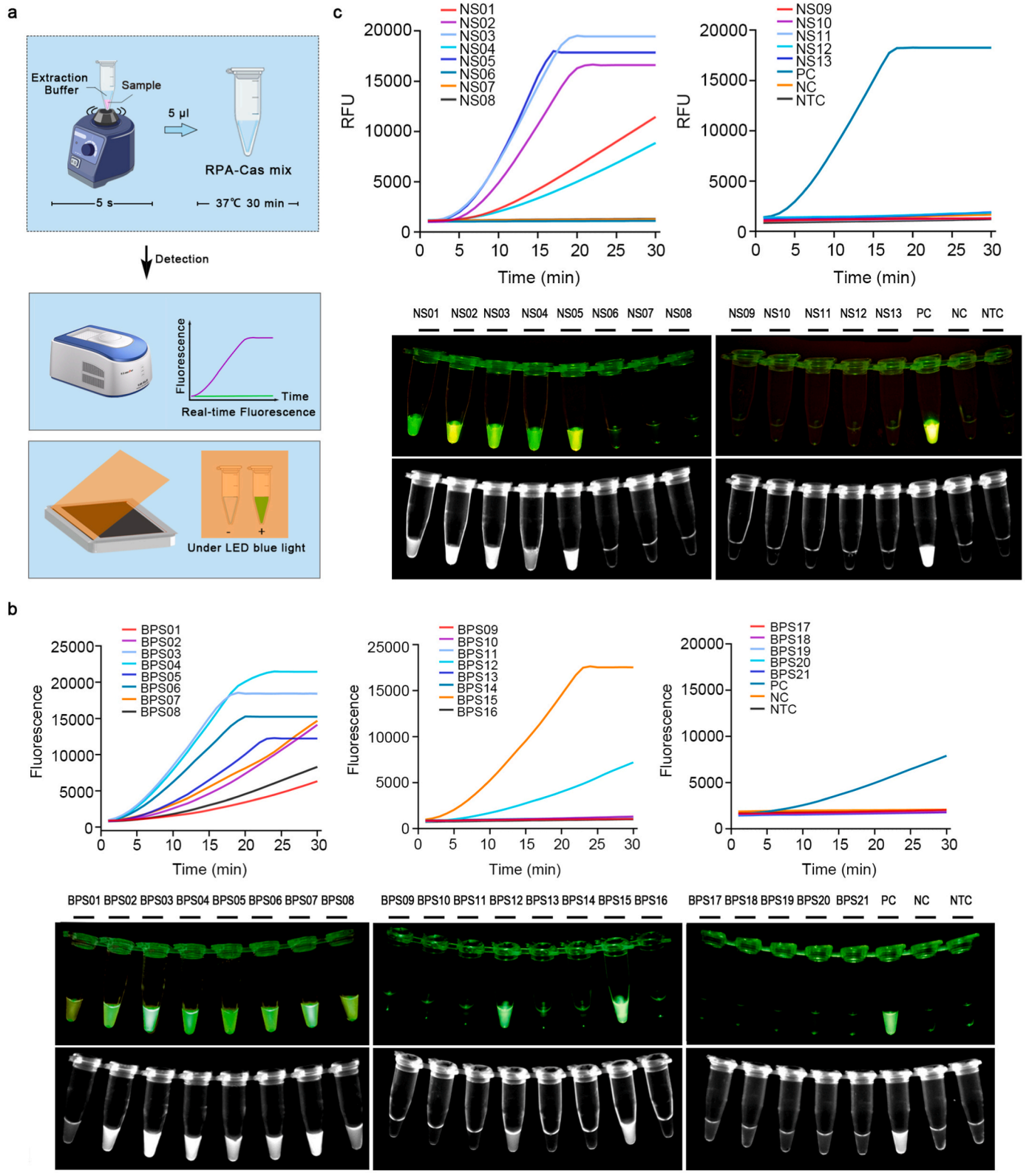


Fig. 6. Detection of clinical swab samples by ORCD and RT-ORCD. a. Schematic showing the ORCD assay system with a nucleic acid extraction-free release agent for rapid and visual nucleic acid detection. The sample was mixed with extraction buffer for a few seconds to release the nucleic acids and used input for the ORCD or RT-ORCD system, which was monitored by real-time fluorescence PCR or naked eye observation of LED blue light. **b.** Real-time ORCD and endpoint images used for the visual detection of 21 *Bordetella pertussis* clinical samples. Positive control (PC), 200 copies/μL of plasmids containing the *B. pertussis*-1663 sequence; BPS01-BPS21, *Bordetella pertussis* clinical sample 1–21; NC, *Bordetella pertussis* negative control; and NTC, nontemplate control reaction. **c.** Real-time RT-ORCD and endpoint images for the visual detection of 13 13 SARS-CoV-2 clinical samples. Positive control (PC), 400 copies/μL of synthetic SARS-CoV-2 N RNA; NS01-NS13, SARS-CoV-2 sample 1–13; NC, SARS-CoV-2 negative control; and NTC, nontemplate control reaction. (For interpretation of the references to colour in this figure legend, the reader is referred to the Web version of this article.)

system undergoes simultaneous for isothermal amplification and CRISPR/Cas12a detection, abrogating the risk of cross contamination. Additionally, the sensitivity of our system in detecting DNA and RNA was 0.2 copies/μL and 0.4 copies/μL, respectively, which is considered single-copy level sensitivity.

The third key advancement of our ORCD system is related to the relatively low Cas12a activity for detecting of nucleic acids. Previous studies have shown that crRNA/LbCas12a targets the PAM sequence (5′-TTTN-3′) with high *cis*-cleavage and *trans*-cleavage efficiency [25,29]. This high *cis*-cleavage and *trans*-cleavage activity, however, likely cleaves all nucleic acids in the ORCD reaction system, inhibiting the reaction. Therefore, crRNA/Cas12a with relatively low activity is key to the successful use of ORCD method. We reduced the *cis*-cleavage and *trans*-cleavage activity of Cas12a by reducing its concentration, and when we used these low concentrations of Cas12a for nucleic acid detection, the sensitivity of the ORCD targeting PAM sequences was greatly improved.

The final key advancement embodied in our ORCD system is performance of viral or bacterial nucleic acid extraction and clinical sample detection within 30 min when the nucleic acid extraction-free release agent method and ORCD (or RT-ORCD) system are used together. Moreover, the results of *B. pertussis* and SARS-CoV-2 detection tests were highly consistent with those obtained with real-time qPCR test results in the clinic, even when samples had very low nucleic acid loads. A recent national survey of more than 19,000 respondents showed that the average waiting time for qPCR test results based on nasal swabs was 4.1 days, and 31% were available only after 4 days and 10% were available only after 10 or more days [39]. These findings clearly illustrate the need of rapid and immediate detection, and the strategy we provide can obtain the detection results within 30 min from sampling to detection. This test can be administered on demand in the clinic without a cumbersome nucleic acid extraction process, providing great convenience for real-time detection.

We have demonstrated that our ORCD (or RT-ORCD) method without PAM limitation is a rapid, one-step, qualitative approach for the visualized detection of DNA or RNA that shows extreme sensitivity and single-base specificity. Furthermore, our simple method for time-saving and visualizing results exhibits great potential for use in the future development of POC molecular diagnostics in the post epidemic era. It can be widely used to quickly detect infectious diseases in unspecialized settings, such as small clinics, airports, fields and other places.

CRediT authorship contribution statement

Kangfeng Lin: Methodology, Data curation, Validation, Writing – original draft. **Jianguang Guo:** Resources, Data curation, Validation. **Xiangju Guo:** Resources, Data curation, Validation. **Qinghan Li:** Resources, Data curation. **Xiao Li:** Resources. **Zhen Sun:** Writing – review & editing. **Zehang Zhao:** Formal analysis. **Jiao Weng:** Resources. **Jinzhun Wu:** Validation, Writing – review & editing. **Rui Zhang:** Conceptualization, Validation, Writing – review & editing. **Boan Li:** Conceptualization, Validation, Writing – review & editing, Supervision.

Declaration of competing interest

The authors declare that they have no known competing financial interests or personal relationships that could have appeared to influence the work reported in this paper.

Data availability

Data will be made available on request.

Acknowledgements

This work was supported by grants from the National Key Research and Development Program of China (2020YFA0112300 to B.-A.L.), the National Natural Science Foundation of China (grant number 81972458 to B.-A.L. 82103092 to R.Z.), the Natural Science Foundation of Fujian Province (grant number 2022J05312 to R.Z.) the Health-Education joint research project of Fujian province (grant numbers 2019-WJ-34 to B.-A.L. and Z.-M.Z.), and “Project 111” sponsored by the State Bureau of Foreign Experts and Ministry of Education (grant number B06016).

Appendix A. Supplementary data

Supplementary data to this article can be found online at https://doi.org/10.1016/j.aca.2023.340938.

References

[1] S. Mattoo, J.D. Cherry, Molecular pathogenesis, epidemiology, and clinical manifestations of respiratory infections due to Bordetella pertussis and other Bordetella subspecies, Clin. Microbiol. Rev. 18 (2) (2005) 326–382.
[2] Y. Bi, Q. Chen, Q. Wang, J. Chen, T. Jin, G. Wong, C. Quan, J. Liu, J. Wu, R. Yin, L. Zhao, M. Li, Z. Ding, R. Zou, W. Xu, H. Li, H. Wang, K. Tian, G. Fu, Y. Huang, A. Shestopalov, S. Li, B. Xu, H. Yu, T. Luo, L. Lu, X. Xu, Y. Luo, Y. Liu, W. Shi, D. Liu, G.F. Gao, Genesis, evolution and prevalence of H5N6 avian influenza viruses in China, Cell Host Microbe 20 (6) (2016) 810–821.
[3] J.K. Taubenberger, A.H. Reid, A.E. Krafft, K.E. Bijwaard, T.G. Fanning, Initial genetic characterization of the 1918 "Spanish" influenza virus, Science 275 (5307) (1997) 1793–1796.
[4] T. Kuiken, R.A. Fouchier, M. Schutten, G.F. Rimmelzwaan, G. Van Amerongen, D. Van Riel, J.D. Laman, T. De Jong, G. Van Doornum, W. Lim, Newly discovered coronavirus as the primary cause of severe acute respiratory syndrome, Lancet 362 (9380) (2003) 263–270.
[5] P. V'Kovski, A. Kratzel, S. Steiner, H. Stalder, V. Thiel, Coronavirus biology and replication: implications for SARS-CoV-2, Nat. Rev. Microbiol. 19 (3) (2021) 155–170.
[6] C. Wang, P.W. Horby, F.G. Hayden, G.F. Gao, A novel coronavirus outbreak of global health concern, Lancet 395 (10223) (2020) 470–473.
[7] N. Zhu, D. Zhang, W. Wang, X. Li, B. Yang, J. Song, X. Zhao, B. Huang, W. Shi, R. Lu, P. Niu, F. Zhan, X. Ma, D. Wang, W. Xu, G. Wu, G.F. Gao, W. Tan, I. China Novel Coronavirus, T. Research, A novel coronavirus from patients with pneumonia in China, 2019, N. Engl. J. Med. 382 (8) (2020) 727–733.
[8] WHO, WHO Coronavirus (COVID-19) Dashboard, 2022. https://covid19.who.int/. 2022.
[9] R.S. Lanciotti, C.H. Calisher, D.J. Gubler, G.-J. Chang, A.V. Vorndam, Rapid detection and typing of dengue viruses from clinical samples by using reverse transcriptase-polymerase chain reaction, J. Clin. Microbiol. 30 (3) (1992) 545–551.
[10] A.M. Wang, M.V. Doyle, D.F. Mark, Quantitation of mRNA by the polymerase chain reaction, Proc. Natl. Acad. Sci. USA 86 (24) (1989) 9717–9721.
[11] M. Vanaerschot, S.A. Mann, J.T. Webber, J. Kamm, S.M. Bell, J. Bell, S.N. Hong, M. P. Nguyen, L.Y. Chan, K.D. Bhatt, Identification of a polymorphism in the N gene of SARS-CoV-2 that adversely impacts detection by reverse transcription-PCR, J. Clin. Microbiol. 59 (1) (2020) e02369-20.
[12] S. Lutz, P. Weber, M. Focke, B. Faltin, J. Hoffmann, C. Muller, D. Mark, G. Roth, P. Munday, N. Armes, O. Piepenburg, R. Zengerle, F. von Stetten, Microfluidic lab-on-a-foil for nucleic acid analysis based on isothermal recombinase polymerase amplification (RPA), Lab Chip 10 (7) (2010) 887–893.
[13] O. Piepenburg, C.H. Williams, D.L. Stemple, N.A. Armes, DNA detection using recombination proteins, PLoS Biol. 4 (7) (2006), e204.
[14] T. Notomi, H. Okayama, H. Masubuchi, T. Yonekawa, K. Watanabe, N. Amino, T. Hase, Loop-mediated isothermal amplification of DNA, Nucleic Acids Res. 28 (12) (2000) e63-e63.
[15] P. Hardinge, J.A.H. Murray, Reduced false positives and improved reporting of loop-mediated isothermal amplification using quenched fluorescent primers, Sci. Rep. 9 (1) (2019) 7400.
[16] J.C. Rolando, E. Jue, J.T. Barlow, R.F. Ismagilov, Real-time kinetics and high-resolution melt curves in single-molecule digital LAMP to differentiate and study specific and non-specific amplification, Nucleic Acids Res. 48 (7) (2020) e42.
[17] C.B.F. Vogels, A.F. Brito, A.L. Wyllie, J.R. Fauver, I.M. Ott, C.C. Kalinich, M. E. Petrone, A. Casanovas-Massana, M. Catherine Muenker, A.J. Moore, J. Klein, P. Lu, A. Lu-Culligan, X. Jiang, D.J. Kim, E. Kudo, T. Mao, M. Moriyama, J.E. Oh, A. Park, J. Silva, E. Song, T. Takahashi, M. Taura, M. Tokuyama, A. Venkataraman, O.E. Weizman, P. Wong, Y. Yang, N.R. Cheemarla, E.B. White, S. Lapidus, R. Earnest, B. Geng, P. Vijayakumar, C. Odio, J. Fournier, S. Bermejo, S. Farhadian, C.S. Dela Cruz, A. Iwasaki, A.I. Ko, M.L. Landry, E.F. Foxman, N.D. Grubaugh, Analytical sensitivity and efficiency comparisons of SARS-CoV-2 RT-qPCR primer-probe sets, Nat Microbiol 5 (10) (2020) 1299–1305.
[18] R. Bruch, G.A. Urban, C. Dincer, CRISPR/Cas powered multiplexed biosensing, Trends Biotechnol. 37 (8) (2019) 791–792.
[19] D.S. Chertow, Next-generation diagnostics with CRISPR, Science 360 (6387) (2018) 381–382.
[20] O.O. Abudayyeh, J.S. Gootenberg, S. Konermann, J. Joung, I.M. Slaymaker, D. B. Cox, S. Shmakov, K.S. Makarova, E. Semenova, L. Minakhin, C2c2 is a single-component programmable RNA-guided RNA-targeting CRISPR effector, Science 353 (6299) (2016) aaf5573.

[21] G. Aquino-Jarquin, CRISPR-Cas14 is now part of the artillery for gene editing and molecular diagnostic, Nanomedicine 18 (2019) 428–431.
[22] P. Fozouni, S. Son, M. Diaz de Leon Derby, G.J. Knott, C.N. Gray, M.V. D'Ambrosio, C. Zhao, N.A. Switz, G.R. Kumar, S.I. Stephens, D. Boehm, C.L. Tsou, J. Shu, A. Bhuiya, M. Armstrong, A.R. Harris, P.Y. Chen, J.M. Osterloh, A. Meyer-Franke, B. Joehnk, K. Walcott, A. Sil, C. Langelier, K.S. Pollard, E.D. Crawford, A. S. Puschnik, M. Phelps, A. Kistler, J.L. DeRisi, J.A. Doudna, D.A. Fletcher, M. Ott, Amplification-free detection of SARS-CoV-2 with CRISPR-Cas13a and mobile phone microscopy, Cell 184 (2) (2021) 323–333 e9.
[23] J.S. Gootenberg, O.O. Abudayyeh, J.W. Lee, P. Essletzbichler, A.J. Dy, J. Joung, V. Verdine, N. Donghia, N.M. Daringer, C.A. Freije, Nucleic acid detection with CRISPR-Cas13a/C2c2, Science 356 (6336) (2017) 438–442.
[24] L. Li, S. Li, N. Wu, J. Wu, G. Wang, G. Zhao, J. Wang, HOLMESv2: a CRISPR-cas12b-assisted platform for nucleic acid detection and DNA methylation quantitation, ACS Synth. Biol. 8 (10) (2019) 2228–2237.
[25] S.Y. Li, Q.X. Cheng, J.K. Liu, X.Q. Nie, G.P. Zhao, J. Wang, CRISPR-Cas12a has both cis- and trans-cleavage activities on single-stranded DNA, Cell Res. 28 (4) (2018) 491–493.
[26] T.Y. Liu, G.J. Knott, D.C.J. Smock, J.J. Desmarais, S. Son, A. Bhuiya, S. Jakhanwal, N. Prywes, S. Agrawal, M.D. de Leon Derby, N.A. Switz, M. Armstrong, A.R. Harris, E.J. Charles, B.W. Thornton, P. Fozouni, J. Shu, S.I. Stephens, G.R. Kumar, C. Zhao, A. Mok, A.T. Iavarone, A.M. Escajeda, R. McIntosh, S.E. Kim, E.J. Dugan, I.G.I. T. Consortium, K.S. Pollard, M.X. Tan, M. Ott, D.A. Fletcher, L.F. Lareau, P.D. Hsu, D.F. Savage, J.A. Doudna, Accelerated RNA detection using tandem CRISPR nucleases, medRxiv 17 (9) (2021) 982–988.
[27] F. Teng, L. Guo, T. Cui, X.G. Wang, K. Xu, Q. Gao, Q. Zhou, W. Li, CDetection: CRISPR-Cas12b-based DNA detection with sub-attomolar sensitivity and single-base specificity, Genome Biol. 20 (1) (2019) 132.
[28] B. Tian, G.A.S. Minero, J. Fock, M. Dufva, M.F. Hansen, CRISPR-Cas12a based internal negative control for nonspecific products of exponential rolling circle amplification, Nucleic Acids Res. 48 (5) (2020) e30.
[29] B. Zetsche, J.S. Gootenberg, O.O. Abudayyeh, I.M. Slaymaker, K.S. Makarova, P. Essletzbichler, S.E. Volz, J. Joung, J. van der Oost, A. Regev, E.V. Koonin, F. Zhang, Cpf1 is a single RNA-guided endonuclease of a class 2 CRISPR-Cas system, Cell 163 (3) (2015) 759–771.
[30] J.S. Gootenberg, O.O. Abudayyeh, M.J. Kellner, J. Joung, J.J. Collins, F. Zhang, Multiplexed and portable nucleic acid detection platform with Cas13, Cas12a, and Csm6, Science 360 (6387) (2018) 439–444.
[31] J.S. Chen, E. Ma, L.B. Harrington, M. Da Costa, X. Tian, J.M. Palefsky, J.A. Doudna, CRISPR-Cas12a target binding unleashes indiscriminate single-stranded DNase activity, Science 360 (6387) (2018) 436–439.
[32] S.Y. Li, Q.X. Cheng, J.M. Wang, X.Y. Li, Z.L. Zhang, S. Gao, R.B. Cao, G.P. Zhao, J. Wang, CRISPR-Cas12a-assisted nucleic acid detection, Cell Discov 4 (2018) 20.
[33] J.P. Broughton, X. Deng, G. Yu, C.L. Fasching, V. Servellita, J. Singh, X. Miao, J. A. Streithorst, A. Granados, A. Sotomayor-Gonzalez, K. Zorn, A. Gopez, E. Hsu, W. Gu, S. Miller, C.Y. Pan, H. Guevara, D.A. Wadford, J.S. Chen, C.Y. Chiu, CRISPR-Cas12-based detection of SARS-CoV-2, Nat. Biotechnol. 38 (7) (2020) 870–874.
[34] M. Patchsung, K. Jantarug, A. Pattama, K. Aphicho, S. Suraritdechachai, P. Meesawat, K. Sappakhaw, N. Leelahakorn, T. Ruenkam, T. Wongsatit, N. Athipanyasilp, B. Eiamthong, B. Lakkanasirorat, T. Phoodokmai, N. Niljianskul, D. Pakotiprapha, S. Chanarat, A. Homchan, R. Tinikul, P. Kamutira, K. Phiwkaow, S. Soithongcharoen, C. Kantiwiriyawanitch, V. Pongsupasa, D. Trisrivirat, J. Jaroensuk, T. Wongnate, S. Maenpuen, P. Chaiyen, S. Kamnerdnakta, J. Swangsri, S. Chuthapisith, Y. Sirivatanauksorn, C. Chaimayo, R. Sutthent, W. Kantakamalakul, J. Joung, A. Ladha, X. Jin, J.S. Gootenberg, O.O. Abudayyeh, F. Zhang, N. Horthongkham, C. Uttamapinant, Clinical validation of a Cas13-based assay for the detection of SARS-CoV-2 RNA, Nat Biomed Eng 4 (12) (2020) 1140–1149.
[35] X. Ding, K. Yin, Z. Li, R.V. Lalla, E. Ballesteros, M.M. Sfeir, C. Liu, Ultrasensitive and visual detection of SARS-CoV-2 using all-in-one dual CRISPR-Cas12a assay, Nat. Commun. 11 (1) (2020) 1–10.
[36] H. de Puig, R.A. Lee, D. Najjar, X. Tan, L.R. Soenksen, N.M. Angenent-Mari, N. M. Donghia, N.E. Weckman, A. Ory, C.F. Ng, Minimally instrumented SHERLOCK (miSHERLOCK) for CRISPR-based point-of-care diagnosis of SARS-CoV-2 and emerging variants, Sci. Adv. 7 (32) (2021), eabh2944.
[37] S. Lu, X. Tong, Y. Han, K. Zhang, Y. Zhang, Q. Chen, J. Duan, X. Lei, M. Huang, Y. Qiu, Fast and sensitive detection of SARS-CoV-2 RNA using suboptimal protospacer adjacent motifs for Cas12a, Nature Biomedical Engineering 6 (3) (2022) 286–297.
[38] E. Toth, E. Varga, P.I. Kulcsar, V. Kocsis-Jutka, S.L. Krausz, A. Nyeste, Z. Welker, K. Huszar, Z. Ligeti, A. Talas, E. Welker, Improved LbCas12a variants with altered PAM specificities further broaden the genome targeting range of Cas12a nucleases, Nucleic Acids Res. 48 (7) (2020) 3722–3733.
[39] D. Lazer, M. Santillana, R.H. Perlis, K. Ognyanova, M.A. Baum, State of the Nation: a 50-state COVID-19 Survey: Report# 8: Failing the Test: Waiting Times for COVID Diagnostic Tests across the US, 2020.